molbank

MDPI

Communication

Synthesis of (Z)-3-Allyl-5-(4-nitrobenzylidene)-2-sulfanylidene-1,3-thiazolidin-4-one and Determination of Its Crystal Structure

Bastien Moreno [1], Isabelle Jourdain [1,*], Michael Knorr [1,*], Sarra Boudriga [2], Carsten Strohmann [3] and Tobias Schrimpf [3]

[1] Institut UTINAM UMR 6213 CNRS, Université de Franche-Comté, 16, Route de Gray, 25030 Besançon, France
[2] Laboratory of Heterocyclic Chemistry Natural Product and Reactivity (LR11ES39), Department of Chemistry, Faculty of Science of Monastir, University of Monastir, Monastir 5019, Tunisia; sarra.boudriga@fsm.rnu.tn
[3] Anorganische Chemie, Technische Universität Dortmund, Otto-Hahn Straße 6, 44227 Dortmund, Germany; carsten.strohmann@tu-dortmund.de (C.S.); tobias.schrimpf@tu-dortmund.de (T.S.)
* Correspondence: isabelle.jourdain@univ-fcomte.fr (I.J.); michael.knorr@univ-fcomte.fr (M.K.); Tel.: +33-3-81-66-62-70 (M.K.)

Abstract: To extend the existing library of arylidenerhodanines which display a potential biological activity, 3-*N*-allylrhodanine **1** was condensed under Knoevenagel conditions with *p*-nitrobenzaldehyde in acetic acid to afford the π-conjugated heterocyclic compound 3-allyl-5-(4-nitrobenzylidene)-2-sulfanylidene-1,3-thiazolidin-4-one **2**. Compound **2** was characterized by IR and NMR spectroscopy, and its UV-vis spectrum was compared with that of compound 3-allyl-5-(4-methoxybenzylidene)-2-sulfanylidene-1,3-thiazolidin-4-one **3.** The molecular structure is ascertained by a single-crystal X-ray diffraction study performed at 100 K.

Keywords: allylrhodanine; thione; crystal structure; UV-vis spectra; Knoevenagel condensation; Hirshfeld analysis

Citation: Moreno, B.; Jourdain, I.; Knorr, M.; Boudriga, S.; Strohmann, C.; Schrimpf, T. Synthesis of (Z)-3-Allyl-5-(4-nitrobenzylidene)-2-sulfanylidene-1,3-thiazolidin-4-one and Determination of Its Crystal Structure. *Molbank* **2024**, *2024*, M1783. https://doi.org/10.3390/M1783

Academic Editor: Fawaz Aldabbagh

Received: 14 February 2024
Revised: 27 February 2024
Accepted: 28 February 2024
Published: 1 March 2024

1. Introduction

The five-membered heterocyclic compound rhodanine, also called 2-thioxo-4-thiazolidinone (see Figure 1) and its derivatives [1] not only play a role in organic chemistry as building blocks for further transformations but have also found application in various therapeutic areas [2,3] due to their broad spectrum of biological and pharmacological activities. These include antidiabetic activity [4], protein kinase inhibitors [5,6], topoisomerase II inhibition potency [7,8], anticancer activity against MCF-7 breast cancer [9,10] and potential cholinesterase inhibitors [11,12]. After approval of the *N*-substituted rhodanine Epalrestat [13] by the Food and Drug Administration (FDA) as an inhibitor drug for the treatment of diabetic neuropathy [14], several arylidene *N*-substituted rhodanine derivatives have also been identified as potential inhibitors of essential therapeutic targets such as PTP1B [15], α-amylase [16] and α-glucosidase [17] for the clinical management of Type 2 diabetes mellitus (T2DM) (Figure 1). Very recently, we successfully synthesized a series of novel dispirooxindoles-based rhodanine derivatives as potent inhibitors against α-amylase enzyme with in vivo hypoglycemic activity [18].

Arylidene-functionalized rhodanines were also recently screened to evaluate their anticancer activity against several cancer cell lines [19,20] or their propensity as antibacterial, antifungal or antioxidants agents [21–23]. In this context, we have reacted a series of 4-arylidene-5-thioxo-thiazolidin-2-ones with the secondary cyclic amine tetrahydroisoquinoline (THIQ) to convert them to (*Z*)-5-ylidene-2-aminothiazol-4(*5H*)-ones [18]. Some selected compounds incorporating the rhodanine motive and displaying a pharmacological activity are presented in Figure 1.

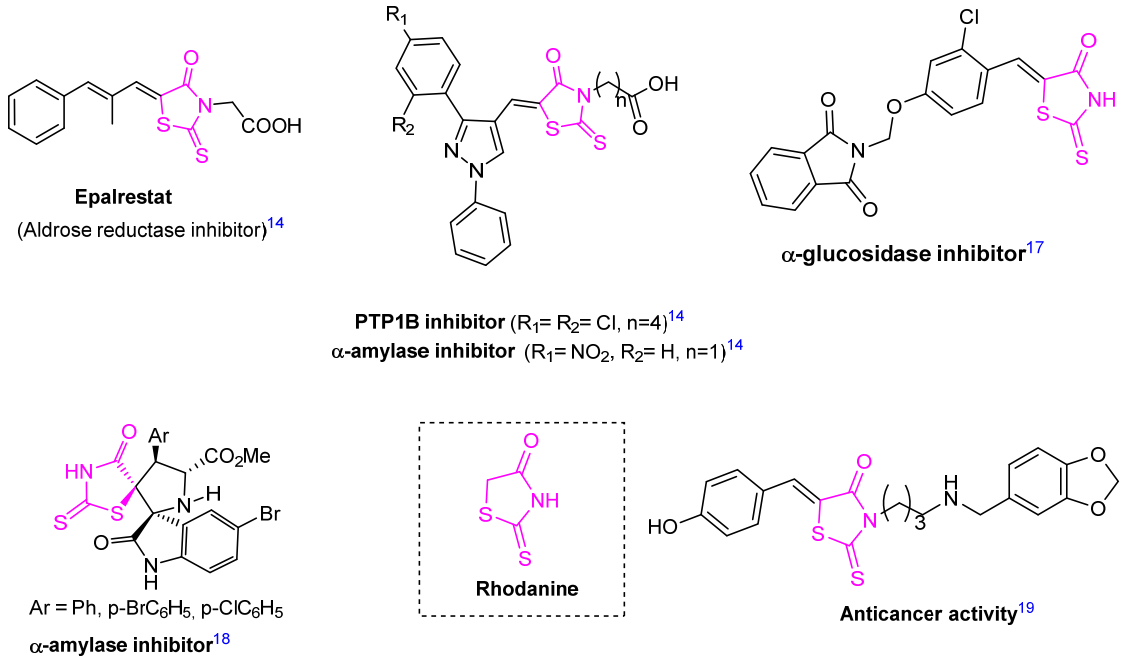

Figure 1. Examples of some rhodanines displaying a biological activity.

Furthermore, rhodanine derivatives attracted the attention of coordination chemists, since the soft C=S thione function (according Pearson's HSAB principle) [24] readily coordinates to a wide range of transition metal complexes producing complexes with Cu(I), Pd(II), Pt(II) etc. [25–28]. The research presented here is (*i*) a continuation of our investigations into the coordination chemistry of thione-type ligand on diverse metal centers [29–33] and (*ii*) the design of novel rhodanine-based scaffolds for probing their biological activities [18].

2. Results and Discussion

The hitherto unknown arylidene rhodanine derivate 3-allyl-5-(4-nitrobenzylidene)-2-sulfanylidene-1,3-thiazolidin-4-one **2** was obtained by addition of *p*-nitrobenzaldehyde to a solution of commercially available *N*-allylrhodanine **1** in acetic acid via a classical Knoevenagel condensation route [34] (Scheme 1). Note that the synthesis of an isomer of **2** bearing the NO_2 group at the meta-position has been described by Ajlaoui et al. by the reaction of *N*-allylrhodanine **1** with (3-nitrobenzylidene)-4-methyl-5-oxopyrazolidin-2-ium ylide [35] and its NH analogue 5-(3-nitrobenzylidene)-2-sulfanylidene-1,3-thiazolidin-4-one has been isolated by Hesse using an L-proline-based deep eutectic solvent [22].

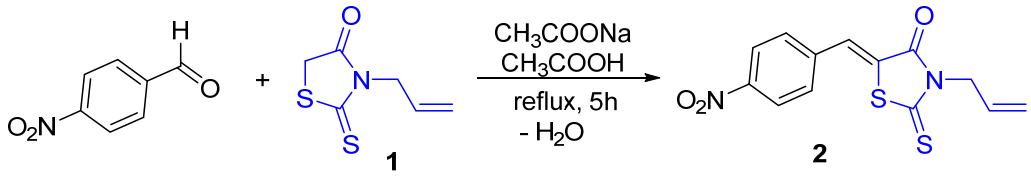

Scheme 1. Knoevenagel synthesis of *N*-allylrhodanine **2**.

The structure of **2** was established using spectroscopic characterization and elemental analysis. On the infrared spectrum, an intense band at 1700 cm^{-1} is associated with the carbonyl group and the thiocarbonyl vibration is observed at 1217 cm^{-1}. The NO stretching bands of the nitro group are located at 1509 and 1327 cm^{-1} and the ν(C=C) appear near 1590 cm^{-1} (see Figure S1). The ^{1}H-NMR recorded in d_6-DMSO (Figure 2) reveals the aryl signals as doublets at δ 7.91 and 8.36 ppm. The chemical shift in the vinyl proton at δ 7.93 indicates that the exocyclic double bond has a *Z*-configuration, as already observed for other 5-arylidene rhodanines described in the literature [6]. Its signal appears at a lower

field than that of the *E*-isomer due to the stronger deshielding effect of the carbonyl group compared to the sulfur atom [36]. Four multiplets between 4.90–5.90 ppm are assigned to the allyl group. A pseudo doublet of triplet is present at δ 4.67 for the NCH_2, resulting from ^3J and ^4J allylic couplings of 5.2 and 1.4 Hz, respectively. The terminal vinyl gives rise to two broad doublets of doublets at δ 5.17 and 5.21 ppm with *trans* and *cis* coupling across the double bond of 17.7 (H1H2) and 10.9 (H'1H2) Hz. The two doublets at δ 5.15 and 5.22 are broad with a small coupling of 1.2 Hz. These apparent quartets result from a ^4J allylic coupling with H3 and a geminal ^2J coupling between H1H'1s with similar values. (Figure 1). The proton decoupled ^{13}C NMR spectrum (Figure 3) reveals the presence of two signals at δ 193.2 and 166.9 ppm attributed to the thiocarbonyl and carbonyl groups of the rhodanine moiety. A resonance at δ 46.7 corresponds to NCH_2, and olefinic carbon appears at 118.4 (C1) and 130.6 (C2, C7).

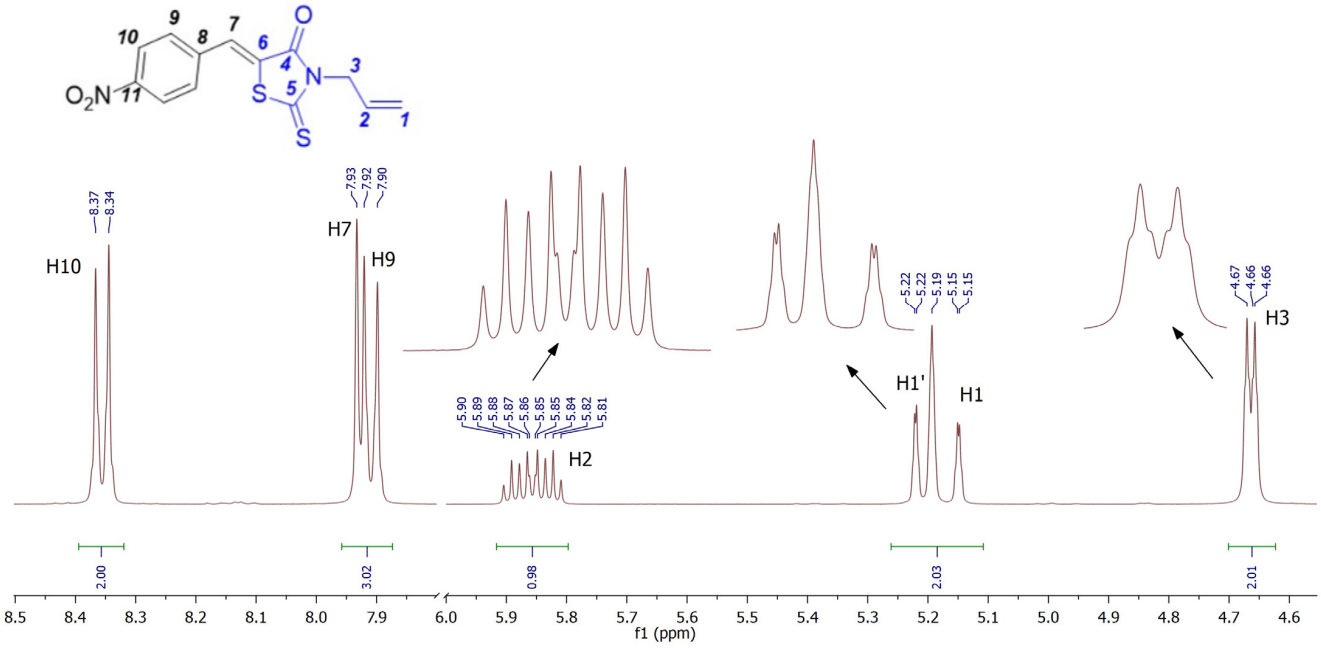

Figure 2. ^1H NMR spectra (400 MHz, DMSO-d_6) of compound **2** at 298 K.

The UV-vis spectrum of highly π-conjugated **2** bearing a strongly electron-withdrawing NO_2-group exerting a -M effect is shown in Figure 4. For comparison, we have also recorded the benzylidene derivative **3** bearing a MeO-group (+M effect) at the *para*-position of the aryl cycle [34]. This literature-known compound has been synthesized using the same experimental procedure described for **2** in 84% yield. The superposition of their UV-vis spectra reveals a bathochromic shift in the absorption bands for **2** compared to **3**, indicating that the NO_2-group causes a diminution in the energetic gap between the frontier orbitals HOMO-LUMO with respect to the methoxy group. The UV-vis spectra recorded in solvents of different polarity are shown in the Supplementary Materials as Figure S2. We tentatively attribute the adsorption bands presented in Table 1 as *n*-π* and π-π* transitions but exclude a push–pull effect despite the strong acceptor propensity of the *p*-nitro group.

Table 1. Absorption data of compounds **2** and **3** in CH_2Cl_2 at 298 K.

Comp.	Absorption: λ_{abs} nm (ε × $10^{-3}M^{-1}cm^{-1}$)
2	239 (5.5), 281 (6.7), 303 sh (4.8), 381 (17.9), 399 sh (16.0)
3	242 (2.8), 262 (3.2), 294 (6.1), 313 sh (3.6), 399 (18.1)

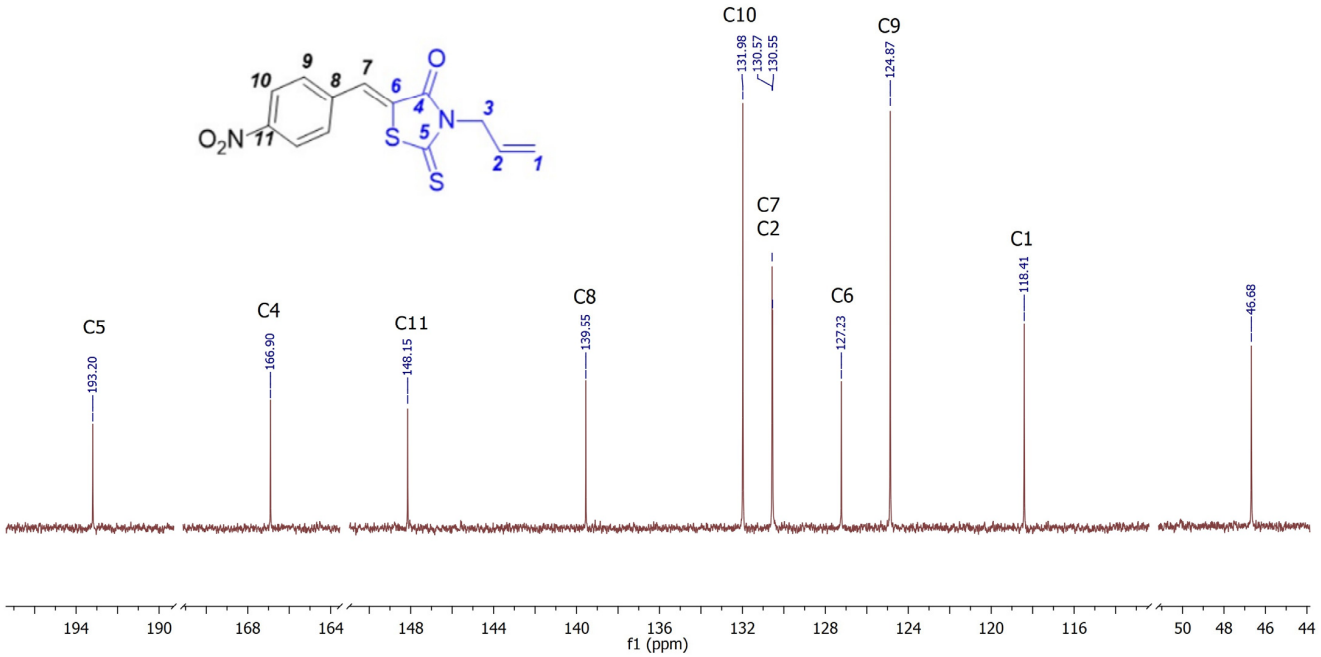

Figure 3. ^{13}C NMR spectra (100 MHz, DMSO-d_6) of compound **2** at 298 K. The DMSO-d_6 signal has been cut off.

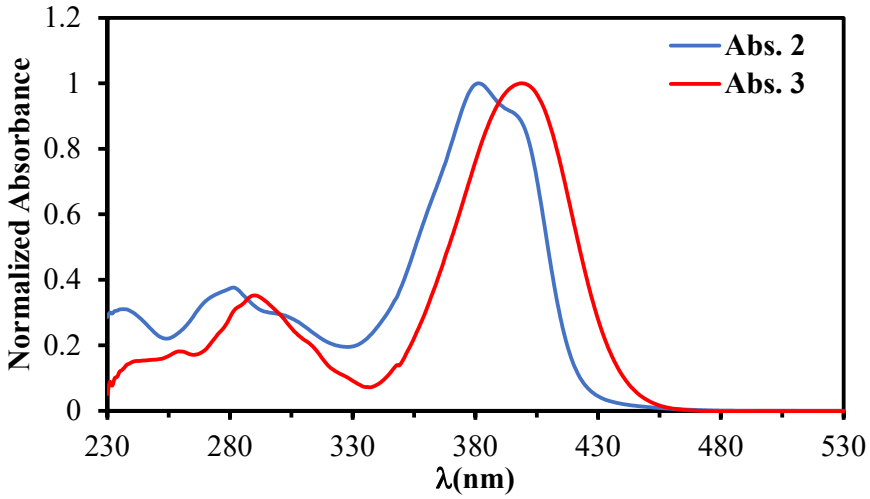

Figure 4. Superposition of the normalized absorption spectra recorded of **2** and **3** in CH_2Cl_2 at 298 K.

To complete the characterization of this compound, we examined **2** crystallizing in the monoclinic space group $P2_1/c$ by an X-ray diffraction study performed at 100 K. As shown in Figure 5, the two cycles linked through the C6=C7 double bond are almost coplanar including the nitro group (torsion angle: 5.81(5)°); the allyl substituent points out of this plane in a perpendicular manner (torsion angle C4N1C1C2 93.6°). The C8 atom of the six-membered benzylidene cycle and the S1 atom are *cis*-arranged with respect to the C6=C7 double bond. Overall, the structure resembles those of other benzylidenerhodanines found in the Cambridge Structural Database (CSD) such as 3-allyl-5-(3-methoxybenzylidene)-2-sulfanylidene-1,3-thiazolidin-4-one (refcod GACVOY) [37], 3-allyl-5-(4-fluorobenzylidene)-2-sulfanylidene-1,3-thiazolidin-4-one (refcod ISAMIA) [38], 3-allyl-5-(4-chlorobenzylidene)-2-sulfanylidene-1,3-thiazolidin-4-one (refcod JADVUI) [39] and 5-benzylidene-3-(prop-2-en-1-yl)-2-sulfanylidene-1,3-thiazolidin-4-one (refcod QIBKOE) [35]. Other crystallographically characterized *N*-allyl rhodanines containing five-membered heterocycles within their framework are 2-thio-3-allyl-5-(2-(3′methylthiazolidinylidene))-thiazolidine-2,4-dione (ref-

cod SALAZO) [40] and (*E*)-3-Allyl-5-(2-thienylmethylene)-2-thioxo-1,3-thiazolidin-4-one (refcod MUGFUR) [41]. Particularly noteworthy is the occurrence of an intramolecular C-H··· S contact between the H9 atom attached at C9 of the aromatic cycle and S1 forming a *pseudo*-six-membered cycle with *d*(C-H ···S) 2.51 Å, with the angle C-H ···S being 133.4°. This kind of contact is also observed in the structures JADVUI (*d*C-H ···S 2.55 Å, angle 133°) and GACVOY (*d*C-H ···S 2.55 Å, angle 133°) [37].

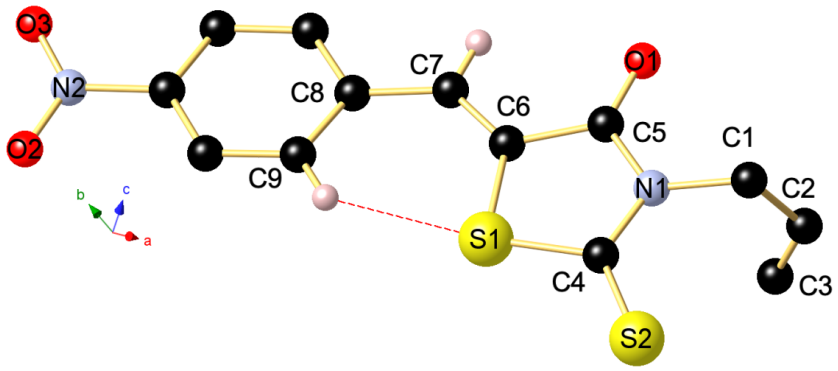

Figure 5. Molecular structure of **2**. Selected bond lengths (Å) and angles (deg) of **2.** Apart from H7 and H9, all other H atoms are omitted for clarity. S1–C6 1.7536(16), S1–C4 1.7614(16), S2–C4 1.6227(16), N1–C4 1.375(2), N1–C1 1.472(2), C1–C2 1.375(2), C2–C3 1.314(3), N1–C5 1.388(2), C5–O12 1.217(2), C5–C6 1.487(2), C6–C7 1.346(2), C7–C8 1.458(2); C3–C2–C1 127.19(16), C2–C1–N1 113.87(14), C1–N1–C4 122.77(14), N1–C4–S2 127.50(13), N1–C4–S1 110.22(11), C4–S1–C6 92.80(8), S1–C6–C5 109.14(11), S1–C6–C7 130.41(12), C6–C5–N1 110.90(13), C6–C7–C8 130.11(14), O2–N2–O3 123.61(14).

In the packing (Figure 6), several secondary weak intermolecular interactions are present such as C-H contacts with the NO_2 group of neighbored molecules (*d*C13-H13. . . O2^{1} 2.505(11) Å, angle 153.4°, symmetry code $^{1}1 + x, y, 1 + z$) and (*d*C3-H3B. . . O3^{2} 2.70(2) Å, angle 162.0°, symmetry code $^{2}1\text{-}x, 1\text{-}y, \text{-}z$). Furthermore, a shorter C-H ···O contact occurs with the carbonyl C=O (*d*C10-H10·····O1^{1} 2.4260(13) Å, angle 130.7°). An intermolecular C-H ···S contact occurs between a CH group of the allyl substituent and the thione function (*d*C2-H2·····S2^{3} 2.9259(5) Å, angle 144.0°, symmetry code $^{3}1 + x, 1/2 - y, -1/2 + z$). As observed for the *p*-chloro derivative [39], the cohesion of the crystal structure also is ensured by an π-π stacking interaction between individual molecules forming inversion dimers. The centroid-to-centroid separation between two stacked benzylidene rings amounts to 3.7986(12) Å (see Figure S3).

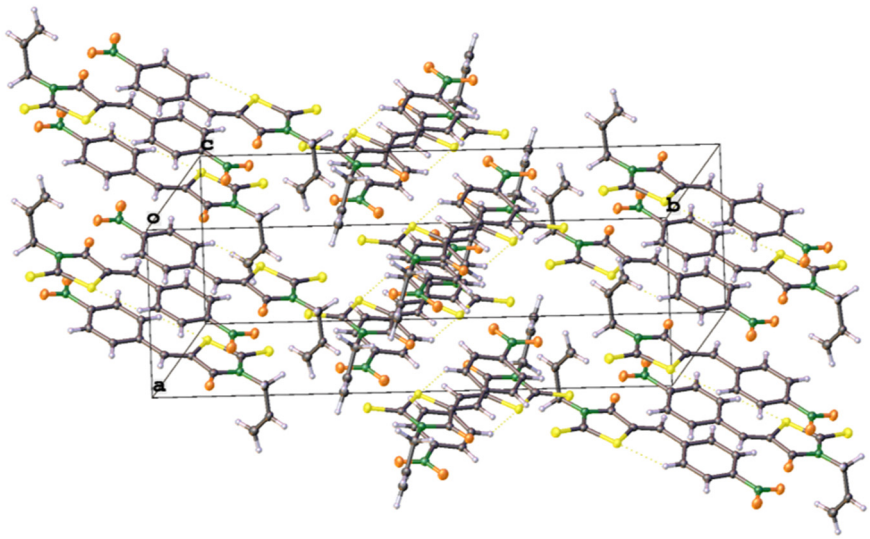

Figure 6. OLEX-generated view of the unit cell of **2** indicating the π—π stacking interaction between individual molecules [42].

These interactions have also been assessed by means of a Hirshfeld surface analysis using the *CrystalExplorer17* software (Figure 7) [43,44]. The Hirshfeld surface was mapped over d_{norm} in the range from –0.2156 to −1.1392 (arbitrary units). The corresponding fingerprints plots are presented in the Supplementary Materials (Figure S4).

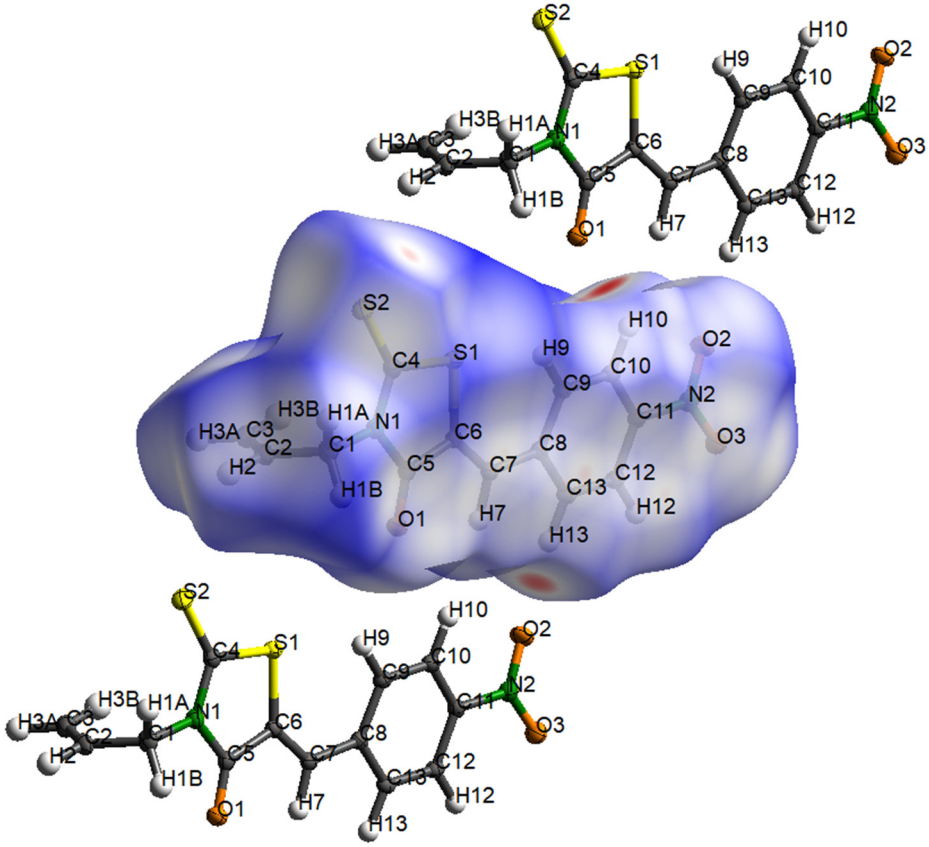

Figure 7. View of the Hirshfeld surface of compound **2** revealing some loose contacts in the crystal structure.

3. Materials and Methods

All reagents were purchased from commercial suppliers and used as received. ^{1}H and ^{13}C NMR spectra were recorded on a Brucker AC 400 (Bruker, Wissembourg, France) spectrometer at 400 and 100 MHz, respectively. The infrared spectrum was recorded on a Vertex 70 spectrometer (Bruker, Wissembourg, France) in ATR mode. UV–Visible spectra were obtained on a VARIAN–Cary 300 array spectrophotometer (Varian, Melbourne, Australia). Elemental analyses were performed on a Thermo Fisher Flashsmart CHNS elemental analyzer.

A mixture of 3-allylrhodanine (1.73 g, 10 mmol), anhydrous sodium acetate (0.82 g, 10 mmol) and 4-nitrobenzaldehyde (1.90 g, 12.5 mmol) was refluxed in 10 mL of glacial acetic acid for 5 h. After cooling, yellow crystals were collected by filtration and washed with H_2O (2 × 5 mL), EtOH (2 × 5 mL) and Et_2O (5 mL). Yield: 95%. Anal. Calc. for $C_{13}H_{10}N_2O_3S_2$ (M.W = 306.37 g.mol^{-1}): C, 50.97; H, 3.29; N, 9.14; S, 20.93%. Found: C, 50.99; H, 3.38; N, 9.28; S, 20.87%. IR-ATR: 1700 ν(C=O), 1217 ν(C=S) cm^{-1}. ^{1}H NMR (DMSO-d_6) at 298 K: δ 4.66 (td, ^{3}J = 5.2, ^{4}J = 1.4, 2H$_3$, NC$\underline{H}_2$), 5.17 (dd, ^{3}J = 17.7, J = 1.2, H1, =C$\underline{H}_2$), 5.21 (dd, ^{3}J = 10.9, J = 1.2, H1′, =C$\underline{H}_2$), 5.85 (tdd, ^{3}J = 17.7, ^{3}J = 10.9, ^{4}J = 5.2, H2, =C$\underline{H}$), 7.91 (d, ^{3}J = 8.82, 2H9, Ar-$\underline{H}$), 7.93 (s, H7, =C$\underline{H}$), 8.35 (d, ^{3}J = 8.82, 2H10, Ar-$\underline{H}$) ppm. ^{13}C NMR (DMSO-d_6) at 298 K: δ 46.7 (C3), 118.4 (C1), 124.9 (C9), 127.2 (C6), 130.5 and 130.6 (C7, C2), 132.0 (C10), 139.6 (C8), 148.2 (C11), 166.9 (C5), 193.2 (C4) ppm.

Since the grown single crystals of **2** used for the determination of the crystal structure were quite small, CuK$_\alpha$ radiation was employed instead of MoK$_\alpha$ radiation. A suitable crys-

tal was mounted on an Bruker APEX-II CCD diffractometer Crystal data for $C_{13}H_{10}N_2O_3S_2$: M = 306.35 g.mol^{-1}, plate-shaped dark yellow crystals, crystal size 0.90 × 0.55 × 0.14 mm^3, monoclinic, space group $P2_1/c$ a = 7.8215(4) Å, b = 26.4778(17) Å, c = 7.1851(4) Å, α = 90°, β = 116.5790(10)°, γ = 90°, V = 1130.75(13) Å^3, Z = 4, D_{calc} = 1.529 g/cm^3, T = 100 K, R_1 = 0.0360, Rw_2 = 0.0966 (all data) for 2726 reflections with I > = 2σ (I) and 2832 independent reflections, GOF = 1.060 Largest diff. peak/hole/e Å^{-3} 0.406/−0.313. The structure was solved using intrinsic phasing and refined using full-matrix least-squares against F^2 (SHELXT, SHELXL 2015) [45,46]. The data were collected using graphite-monochromated CuK_α radiation l = 1.54178 Å and have been deposited at the Cambridge Crystallographic Data Centre as CCDC 2327984. (Supplementary Materials). The data can be obtained free of charge from the Cambridge Crystallographic Data Centre via http://www.ccdc.cam.ac.uk/getstructures.

4. Conclusions

We have shown that arylidenerhodanine **2** is easily accessible in high yields and crystallographically evidenced that this π-conjugated heterocycle features both intra- and intermolecular secondary interactions. We are currently exploring the propensity of this compound to act as an *S*-donor ligand in coordination chemistry.

Supplementary Materials: CIF file, Check-CIF report, UV-Vis and IR spectra and Hirshfeld fingerprint plots. Figures S1–S4.

Author Contributions: B.M. prepared the compound; C.S. and T.S. collected the X-ray data and solved the structure; I.J., S.B. and M.K. designed the study and analyzed the data and wrote the paper. All authors have read and agreed to the published version of the manuscript.

Funding: This research was funded by the Région Bourgogne-Franche-Comté, DeCOmAB project.

Data Availability Statement: The X-ray data are deposited at CCDC as stated in the paper.

Acknowledgments: We thank Stéphanie Beffy for recording the IR and NMR spectra and Abderrahim Khatyr for recording the UV-vis spectra.

Conflicts of Interest: The authors declare no conflicts of interest.

References

1. Brown, F.C.; Bradsher, C.K.; Bond, S.M.; Potter, M. Rhodanine Derivatives. *J. Am. Chem. Soc.* **1951**, *73*, 2357–2359. [CrossRef]
2. Kaminskyy, D.; Kryshchyshyn, A.; Lesyk, R. Recent Developments with Rhodanine as a Scaffold for Drug Discovery. *Expert Opin. Drug Discov.* **2017**, *12*, 1233–1252. [CrossRef]
3. Mousavi, S.M.; Zarei, M.; Hashemi, S.A.; Babapoor, A.; Amani, A.M. A Conceptual Review of Rhodanine: Current Applications of Antiviral Drugs, Anticancer and Antimicrobial Activities. *Artif. Cells Nanomed. Biotechnol.* **2019**, *47*, 1132–1148. [CrossRef] [PubMed]
4. Bin Ahmad Kamar, A.K.D.; Ju Yin, L.; Tze Liang, C.; Tjin Fung, G.; Avupati, V.R. Rhodanine Scaffold: A Review of Antidiabetic Potential and Structure–Activity Relationships (SAR). *Med. Drug Discov.* **2022**, *15*, 100131. [CrossRef]
5. Naufal, M.; Hermawati, E.; Syah, Y.M.; Hidayat, A.T.; Hidayat, I.W.; Al-Anshori, J. Structure–Activity Relationship Study and Design Strategies of Hydantoin, Thiazolidinedione, and Rhodanine-Based Kinase Inhibitors: A Two-Decade Review. *ACS Omega* **2024**, *9*, 4186–4209. [CrossRef] [PubMed]
6. Bourahla, K.; Guihéneuf, S.; Limanton, E.; Paquin, L.; Le Guével, R.; Charlier, T.; Rahmouni, M.; Durieu, E.; Lozach, O.; Carreaux, F.; et al. Design and Microwave Synthesis of New (5Z) 5-Arylidene-2-Thioxo-1,3-Thiazolinidin-4-One and (5Z) 2-Amino-5-Arylidene-1,3-Thiazol-4(5H)-One as New Inhibitors of Protein Kinase DYRK1A. *Pharmaceuticals* **2021**, *14*, 1086. [CrossRef] [PubMed]
7. Khodair, A.I.; Alzahrani, F.M.; Awad, M.K.; Al-Issa, S.A.; Al-Hazmi, G.H.; Nafie, M.S. Design, Synthesis, Computational Investigations, and Antitumor Evaluation of *N*-Rhodanine Glycosides Derivatives as Potent DNA Intercalation and Topo II Inhibition against Cancer Cells. *ACS Omega* **2023**, *8*, 13300–13314. [CrossRef]
8. Jiang, H.; Zhang, W.-J.; Li, P.-H.; Wang, J.; Dong, C.-Z.; Zhang, K.; Chen, H.-X.; Du, Z.-Y. Synthesis and Biological Evaluation of Novel Carbazole-Rhodanine Conjugates as Topoisomerase II Inhibitors. *Bioorg. Med. Chem. Lett.* **2018**, *28*, 1320–1323. [CrossRef] [PubMed]
9. Szczepański, J.; Tuszewska, H.; Trotsko, N. Anticancer Profile of Rhodanines: Structure–Activity Relationship (SAR) and Molecular Targets—A Review. *Molecules* **2022**, *27*, 3750. [CrossRef]

10. Yin, L.J.; Bin Ahmad Kamar, A.K.D.; Fung, G.T.; Liang, C.T.; Avupati, V.R. Review of Anticancer Potentials and Structure-Activity Relationships (SAR) of Rhodanine Derivatives. *Biomed. Pharmacother.* **2022**, *145*, 112406. [CrossRef]
11. Krátký, M.; Nováčková, K.; Svrčková, K.; Švarcová, M.; Štěpánková, Š. New 3-Amino-2-Thioxothiazolidin-4-One-Based Inhibitors of Acetyl- and Butyryl-Cholinesterase: Synthesis and Activity. *Future Med. Chem.* **2024**, *16*, 59–74. [CrossRef]
12. Krátký, M.; Štěpánková, Š.; Vorčáková, K.; Vinšová, J. Synthesis and in Vitro Evaluation of Novel Rhodanine Derivatives as Potential Cholinesterase Inhibitors. *Bioorg. Chem.* **2016**, *68*, 23–29. [CrossRef] [PubMed]
13. Available online: https://en.wikipedia.org/wiki/epalrestat (accessed on 9 February 2024).
14. Hotta, N.; Sakamoto, N.; Shigeta, Y.; Kikkawa, R.; Goto, Y. Clinical Investigation of Epalrestat, an Aldose Reductase Inhibitor, on Diabetic Neuropathy in Japan: Multicenter Study. *J. Diabetes Complicat.* **1996**, *10*, 168–172. [CrossRef] [PubMed]
15. Sun, L.; Wang, P.; Xu, L.; Gao, L.; Li, J.; Piao, H. Discovery of 1,3-Diphenyl-1H-Pyrazole Derivatives Containing Rhodanine-3-Alkanoic Acid Groups as Potential PTP1B Inhibitors. *Bioorg. Med. Chem. Lett.* **2019**, *29*, 1187–1193. [CrossRef] [PubMed]
16. Bansal, G.; Singh, S.; Monga, V.; Thanikachalam, P.V.; Chawla, P. Synthesis and Biological Evaluation of Thiazolidine-2,4-Dione-Pyrazole Conjugates as Antidiabetic, Anti-Inflammatory and Antioxidant Agents. *Bioorg. Chem.* **2019**, *92*, 103271. [CrossRef] [PubMed]
17. Wang, G.; Peng, Y.; Xie, Z.; Wang, J.; Chen, M. Synthesis, α-Glucosidase Inhibition and Molecular Docking Studies of Novel Thiazolidine-2,4-Dione or Rhodanine Derivatives. *Med. Chem. Commun.* **2017**, *8*, 1477–1484. [CrossRef] [PubMed]
18. Toumi, A.; Boudriga, S.; Hamden, K.; Sobeh, M.; Cheurfa, M.; Askri, M.; Knorr, M.; Strohmann, C.; Brieger, L. Synthesis, Antidiabetic Activity and Molecular Docking Study of Rhodanine-Substitued Spirooxindole Pyrrolidine Derivatives as Novel α-Amylase Inhibitors. *Bioorg. Chem.* **2021**, *106*, 104507. [CrossRef]
19. Dago, C.; Ambeu, C.; Coulibaly, W.-K.; Békro, Y.-A.; Mamyrbékova, J.; Defontaine, A.; Baratte, B.; Bach, S.; Ruchaud, S.; Guével, R.; et al. Synthetic Development of New 3-(4-Arylmethylamino)Butyl-5-Arylidene-Rhodanines under Microwave Irradiation and Their Effects on Tumor Cell Lines and against Protein Kinases. *Molecules* **2015**, *20*, 12412–12435. [CrossRef]
20. Ali Muhammad, S.; Ravi, S.; Thangamani, A. Synthesis and Evaluation of Some Novel N-Substituted Rhodanines for Their Anticancer Activity. *Med. Chem. Res.* **2016**, *25*, 994–1004. [CrossRef]
21. Akhavan, M.; Foroughifar, N.; Pasdar, H.; Bekhradnia, A. Green Synthesis, Biological Activity Evaluation, and Molecular Docking Studies of Aryl Alkylidene 2, 4-Thiazolidinedione and Rhodanine Derivatives as Antimicrobial Agents. *Comb. Chem. High Throughput Screen.* **2020**, *22*, 716–727. [CrossRef] [PubMed]
22. Tomašić, T.; Zidar, N.; Mueller-Premru, M.; Kikelj, D.; Mašič, L.P. Synthesis and Antibacterial Activity of 5-Ylidenethiazolidin-4-Ones and 5-Benzylidene-4,6-Pyrimidinediones. *Eur. J. Med. Chem.* **2010**, *45*, 1667–1672. [CrossRef]
23. Hesse, S. Synthesis of 5-Arylidenerhodanines in L-Proline-Based Deep Eutectic Solvent. *Beilstein J. Org. Chem.* **2023**, *19*, 1537–1544. [CrossRef] [PubMed]
24. Pearson, R.G. Recent Advances in the Concept of Hard and Soft Acids and Bases. *J. Chem. Educ.* **1987**, *64*, 561. [CrossRef]
25. Moers, F.G.; Bosman, W.P.J.H.; Beurskens, P.T. Crystal Structure of 3-Methylrhodaninecopper(I) Iodide. *J. Cryst. Mol. Struct.* **1972**, *2*, 23–29. [CrossRef]
26. Moers, F.G.; Goossens, J.W.M.; Langhout, J.P.M. Rhodanine Complexes of Copper(I), Palladium(II) and Platinum(II). *J. Inorg. Nucl. Chem.* **1973**, *35*, 855–859. [CrossRef]
27. Moers, F.G.; Smits, J.M.M.; Beurskens, P.T. Crystal Structure of Bis-(Rhodanine)Copper(I) Iodide, C6H6CuIN2O2S4. *J. Crystallogr. Spectrosc. Res.* **1986**, *16*, 101–106. [CrossRef]
28. Fabretti, A.C.; Peyronel, G.; Franchini, G.C. Copper(I) Complexes of Rhodanine. *Transit. Met. Chem.* **1978**, *3*, 125–127. [CrossRef]
29. Arar, W.; Khatyr, A.; Knorr, M.; Brieger, L.; Krupp, A.; Strohmann, C.; Efrit, M.L.; Ben Akacha, A. Synthesis, Crystal Structures and Hirshfeld Analyses of Phosphonothioamidates $(EtO)_2P(=O)C(=S)N(H)R$ (R = Cy, Bz) and Their Coordination on CuI and HgX_2 (X = Br, I). *Phosphorus Sulfur Silicon Relat. Elem.* **2021**, *196*, 845–858. [CrossRef]
30. Hameau, A.; Guyon, F.; Knorr, M.; Enescu, M.; Strohmann, C. Self-Assembly of Dithiolene-Based Coordination Polymers of Mercury(II): Dithioether versus Thiocarbonyl Bonding. *Monatsh. Chem.* **2006**, *137*, 545–555. [CrossRef]
31. Guyon, F.; Hameau, A.; Khatyr, A.; Knorr, M.; Amrouche, H.; Fortin, D.; Harvey, P.D.; Strohmann, C.; Ndiaye, A.L.; Huch, V.; et al. Syntheses, Structures, and Photophysical Properties of Mono- and Dinuclear Sulfur-Rich Gold(I) Complexes. *Inorg. Chem.* **2008**, *47*, 7483–7492. [CrossRef]
32. Hameau, A.; Guyon, F.; Khatyr, A.; Knorr, M.; Strohmann, C. 4,5-Bis(Methylthio)-1,3-Dithiole-2-Thione, a Versatile Sulphur-Rich Building Block for the Self-Assembly of Cu(I) and Ag(I) Coordination Polymers: Dithioether versus Thiocarbonyl Bonding. *Inorg. Chim. Acta* **2012**, *388*, 60–70. [CrossRef]
33. Arar, W.; Viau, L.; Jourdain, I.; Knorr, M.; Strohmann, C.; Scheel, R.; Ben Akacha, A. Synthesis of Catena-Bis(μ-Bromo)-(*O*-Methyl-N-Phenylthiocarbamate)-Dicopper(I) and Its Reactivity towards PAr_3 (Ar = Ph, p-Tol). *Molbank* **2023**, *2023*, M1655. [CrossRef]
34. Gouveia, F.L.; De Oliveira, R.M.B.; De Oliveira, T.B.; Da Silva, I.M.; Do Nascimento, S.C.; De Sena, K.X.F.R.; De Albuquerque, J.F.C. Synthesis, Antimicrobial and Cytotoxic Activities of Some 5-Arylidene-4-Thioxo-Thiazolidine-2-Ones. *Eur. J. Med. Chem.* **2009**, *44*, 2038–2043. [CrossRef] [PubMed]
35. El Ajlaoui, R.; Ouafa, A.; Mojahidi, S.; El Ammari, L.; Saadi, M.; El Mostapha, R. Unexpected Synthesis of Novel 3-Allyl-5-(Arylidene)-2-Thioxo-Thiazolidin-4-Ones in Reactions of 3-Allylrhodanine with 2-Arylidene-4-Methyl-5-Oxopyrazolidinium Ylides. *Synth. Commun.* **2015**, *45*, 2035–2042. [CrossRef]

36. Momose, Y.; Meguro, K.; Ikeda, H.; Hatanaka, C.; Oi, S.; Sohda, T. Studies on Antidiabetic Agents. X. Synthesis and Biological Activities of Pioglitazone and Related Compounds. *Chem. Pharm. Bull.* **1991**, *39*, 1440–1445. [CrossRef]
37. El Ajlaoui, R.; Rakib, E.M.; Mojahidi, S.; Saadi, M.; El Ammari, L. (*Z*)-3-Allyl-5-(3-Methoxybenzylidene)-2-Sulfanylidene-1,3-Thiazolidin-4-One. *IUCrData* **2016**, *1*, x160052. [CrossRef]
38. El Ajlaoui, R.; Belkhouya, N.; Rakib, E.M.; Mojahidi, S.; Saadi, M.; El Ammari, L. (*Z*)-3-Allyl-5-(4-Fluorobenzylidene)-2-Sulfanylidenethiazolidin-4-one. *IUCrData* **2016**, *1*, x161236. [CrossRef]
39. El Ajlaoui, R.; Rakib, E.M.; Mojahidi, S.; Saadi, M.; El Ammari, L. Crystal Structure of (*Z*)-3-Allyl-5-(4-Chlorobenzylidene)-2-Sulfanylidene-1,3-Thiazolidin-4-one. *Acta Crystallogr. Sect. E Crystallogr. Commun.* **2015**, *71*, o1012. [CrossRef]
40. Germain, G.; Piret, P.; Van Meersche, M.; De Kerf, J. Structure d'une Mérocyanine: $C_{10}H_{12}S_3N_2O$. *Acta Crystallogr.* **1962**, *15*, 373–382. [CrossRef]
41. El Ajlaoui, R.; Rakib, E.M.; Mojahidi, S.; Saadi, M.; El Ammari, L. Crystal Structure of (*E*)-3-Allyl-2-Sulfanylidene-5-[(Thiophen-2-Yl)Methylidene]Thiazolidin-4-one. *Acta Crystallogr. Sect. E Crystallogr. Commun.* **2015**, *71*, o433–o434. [CrossRef]
42. Dolomanov, O.V.; Bourhis, L.J.; Gildea, R.J.; Howard, J.A.K.; Puschmann, H. OLEX2: A complete structure solution, refinement and analysis program. *J. Appl. Crystallogr.* **2009**, *42*, 339–341. [CrossRef]
43. Spackman, M.A.; Jayatilaka, D. Hirshfeld Surface Analysis. *CrystEngComm* **2009**, *11*, 19–32. [CrossRef]
44. Spackman, P.R.; Turner, M.J.; McKinnon, J.J.; Wolff, S.K.; Grimwood, D.J.; Jayatilaka, D.; Spackman, M.A. *CrystalExplorer*: A Program for Hirshfeld Surface Analysis, Visualization and Quantitative Analysis of Molecular Crystals. *J. Appl. Crystallogr.* **2021**, *54*, 1006–1011. [CrossRef] [PubMed]
45. Sheldrick, G.M. Crystal Structure Refinement with *SHELXL*. *Acta Crystallogr. C Struct. Chem.* **2015**, *71*, 3–8. [CrossRef]
46. Sheldrick, G.M. *SHELXT*—Integrated Space-Group and Crystal-Structure Determination. *Acta Crystallogr. A Found Adv.* **2015**, *71*, 3–8. [CrossRef]